Molecular Spectroscopy

Chapter 16

Raman Spectrometry

Instrumental Analysis

Ingle & Crouch

By : Masdarolomoor

Optical Interactions

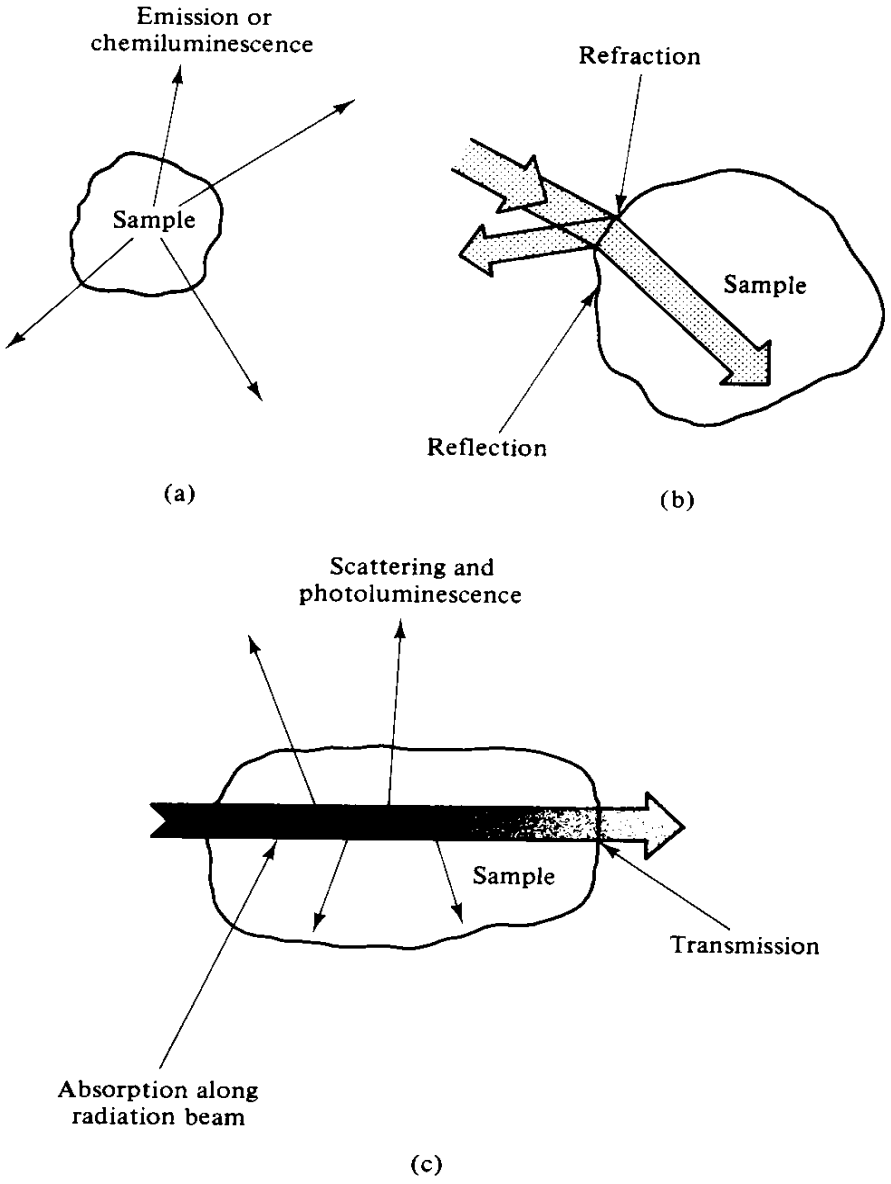

FIGURE 1-1 Some types of optical interactions.

Scattering

Many scattering processes involve no change in the energy of the scattered beam compared to the incident beam. On the surface, these processes appear merely to randomize the direction of an incident beam of photons.

two general classes of scattering phenomena: elastic scattering, in which the scattered radiation is of the same frequency as the incident radiation, and inelastic scattering, in which the scattered radiation is of a different frequency.

Elastic Scattering

TABLE 16-1

Scattering classes

Type of scattering	Refractive index requirement[a]	Size requirement[b]
Rayleigh	$\lvert(\eta_r - 1)\rvert << 1$	$d_s < 0.05\ \lambda$
Debye	$\lvert(\eta_r - 1)\rvert \approx 0.1$	$0.05\ \lambda < d_s < \lambda$
Mie	$(\eta_r - 1) >> 0$	$d_s > \lambda$

[a] η_r, Relative refractive index, η_s/η_m; η_s, refractive index of scatterer; η_m, refractive index of medium.

[b] d_s, Major dimension of scatterer.

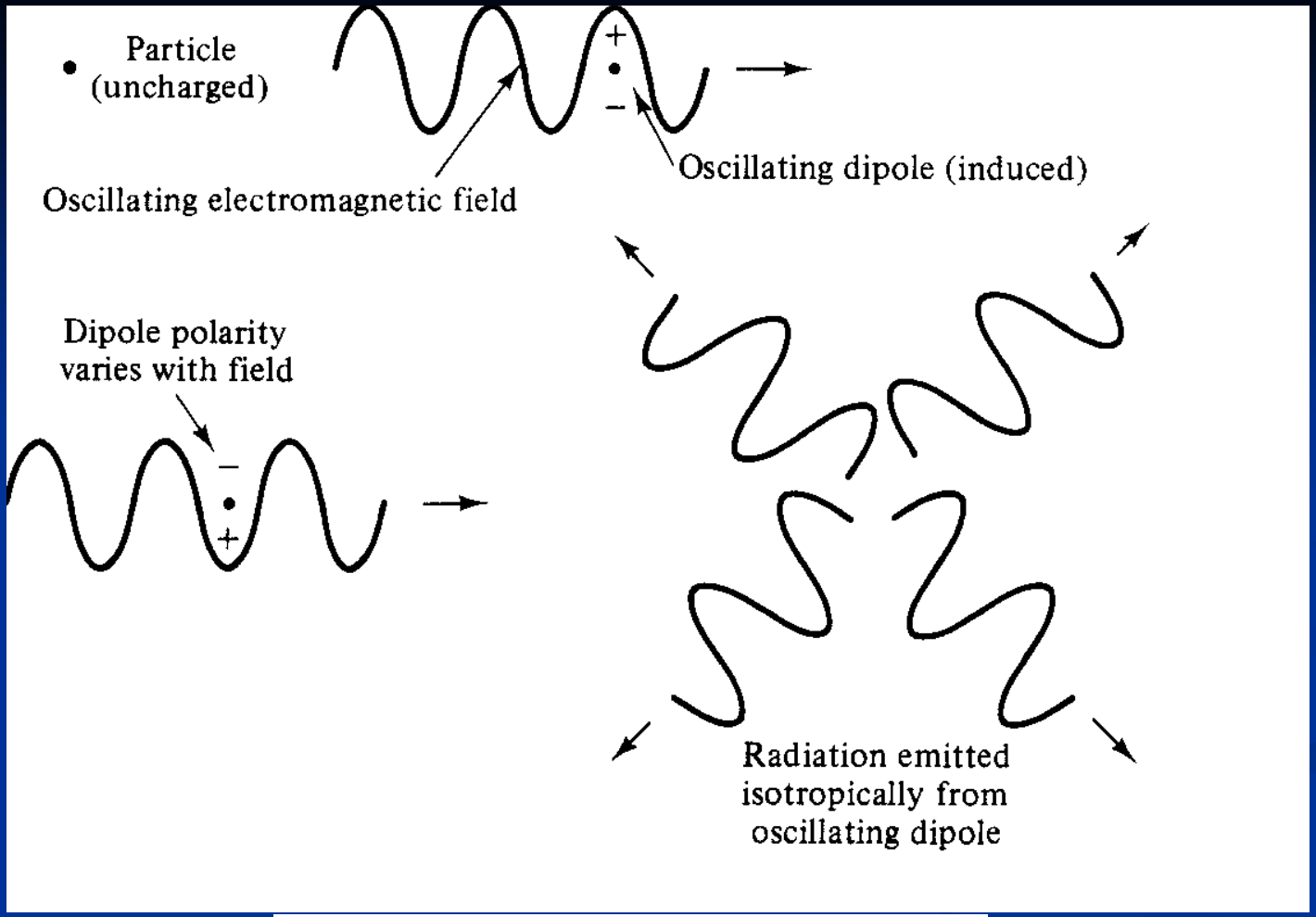

FIGURE 16-1 Schematic diagram illustrating elastic scattering. The oscillating dipole induced in the particle behaves as a secondary source to produce scattered radiation of the same frequency as that incident on the particle.

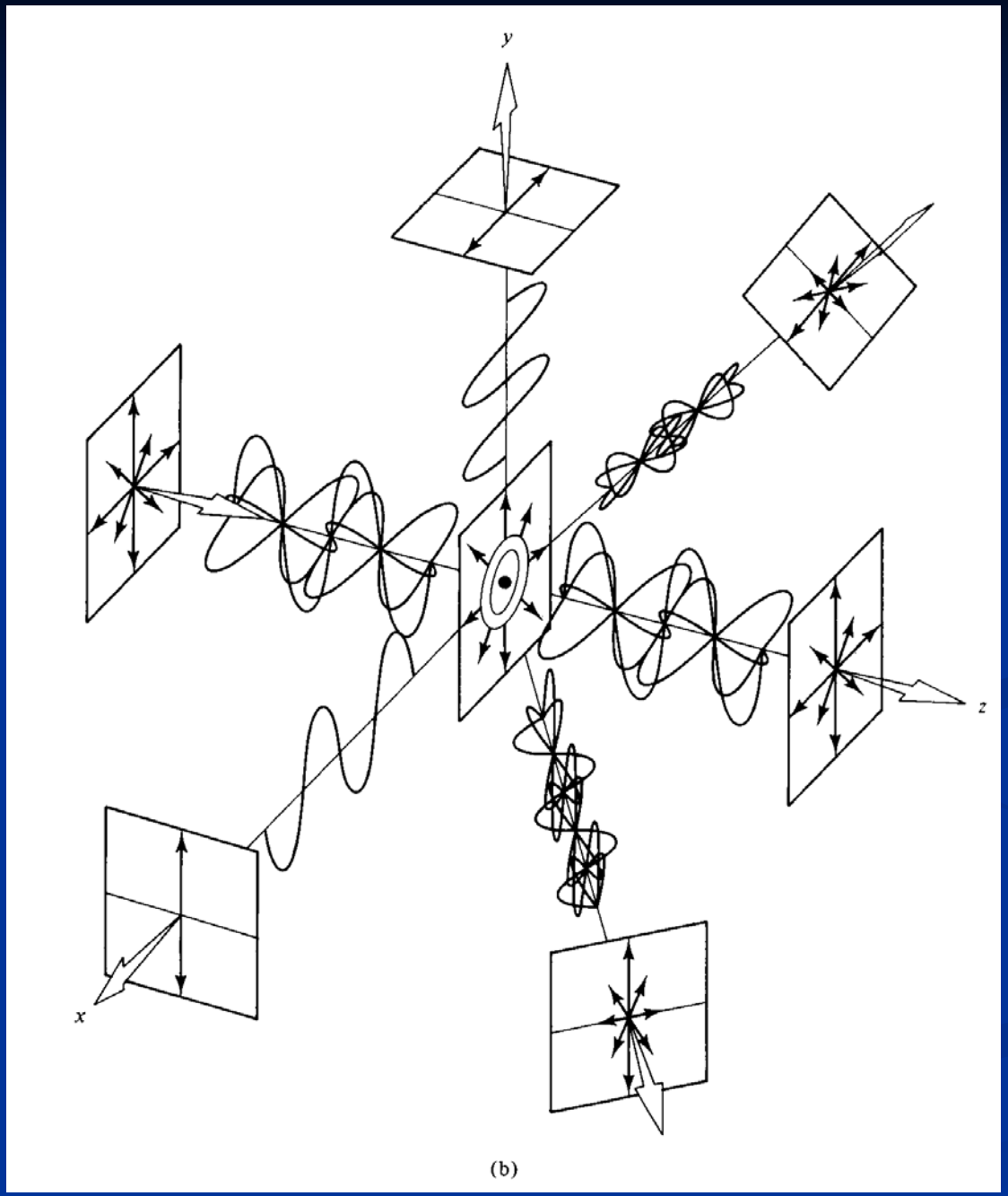

FIGURE 16-2 Scattering of unpolarized monochromatic light by a small spherical particle. The particle is shown at the origin of the axes. In (a) the scattered radiation intensity at a given angle is indicated by the length of the vectors. The envelope represents the cross sections of scattering in the *yz* and the *xy* planes. In (b) the state of polarization of the scattered rays is indicated by the vectors. Radiation scattered in either direction along the *z* axis is unpolarized; off that axis it is partially polarized. When the direction of observation is at 90° to the direction of propagation, the radiation is completely linearly polarized.

Large particle scattering?

The irradiance of the scattered radiation at angle θ, $(E_{sc})_\theta$, is given by

$$(E_{sc})_\theta = \frac{8\pi^4(\alpha')^2(1 + \cos^2\theta)E_0}{\lambda^4 d^2} \qquad (16\text{-}1)$$

where α' is the polarizability of the particle in m^3, λ is the wavelength of the incident radiation, θ is the angle between the incident and scattered ray, E_0 is the incident beam irradiance, and d is the distance from the center of scattering to the detector. The polarizability is a measure of how efficiently a given incident frequency induces a dipole in the particle. Because the polarizability varies roughly with the volume of the scattering particle, equation 16-1 predicts that the scattered radiation intensity increases with increasing particle size. Thus, in a sample that contains particles of various sizes, the larger particles tend to contribute most heavily to the scattering.

Scattering, examples

The sky appears blue because short wavelengths of sunlight are efficiently scattered by small dust particles and water vapor in the atmosphere. The red color of the sun as seen through haze, smoke, or fog results from the efficient transmission of the longer wavelengths of sunlight relative to the shorter wavelengths which are effectively scattered.

Inelastic Scattering

Two types of **inelastic scattering** can be distinguished. In Raman scattering, relatively large frequency shifts occur that are independent of scattering angle. **Raman scattering** is caused by rotational and vibrational transitions in molecules. In addition, scattering can occur with a relatively small frequency shift that varies with the scattering angle. This type of scattering, caused by thermal fluctuations in the medium, is known as **Brillouin scattering**.

Raman Spectroscopy

Raman spectroscopy is the measurement of the wavelength and intensity of inelastically scattered light from molecules. The Raman scattered light occurs at wavelengths that are shifted from the incident light by the energies of molecular vibrations. The mechanism of Raman scattering is different from that of infrared absorption, and Raman and IR spectra provide complementary information. Typical applications are in structure determination, multicomponent qualitative analysis, and quantitative analysis.

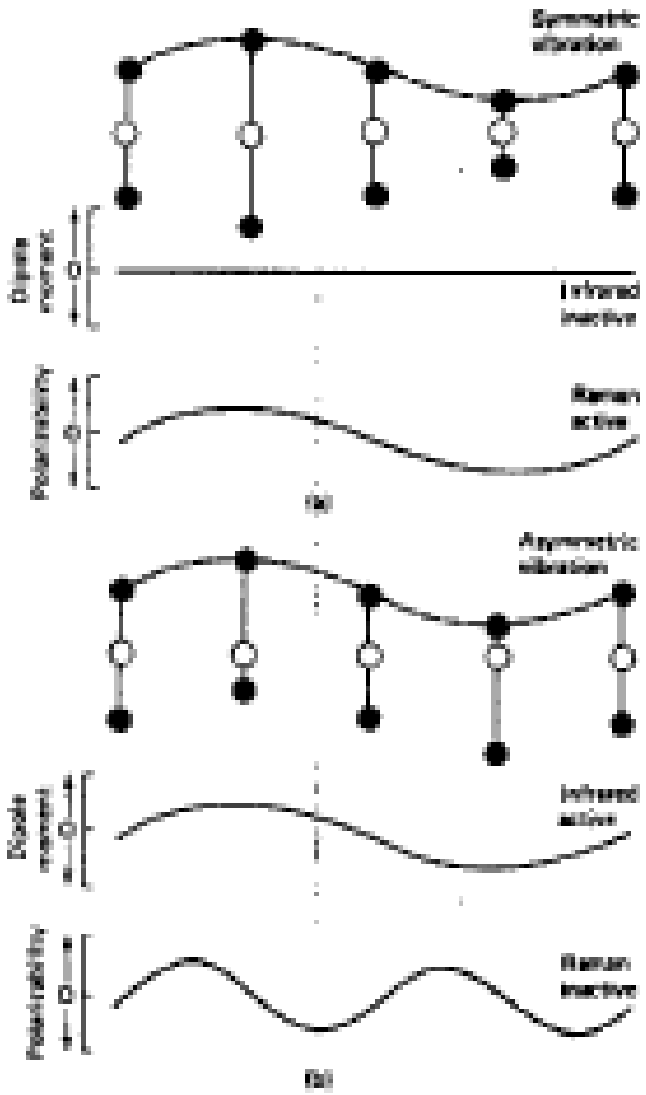

FIGURE 9-4 Raman and infrared activity of two vibrational modes of carbon dioxide: (a) symmetric, (b) asymmetric.

Skoog, West

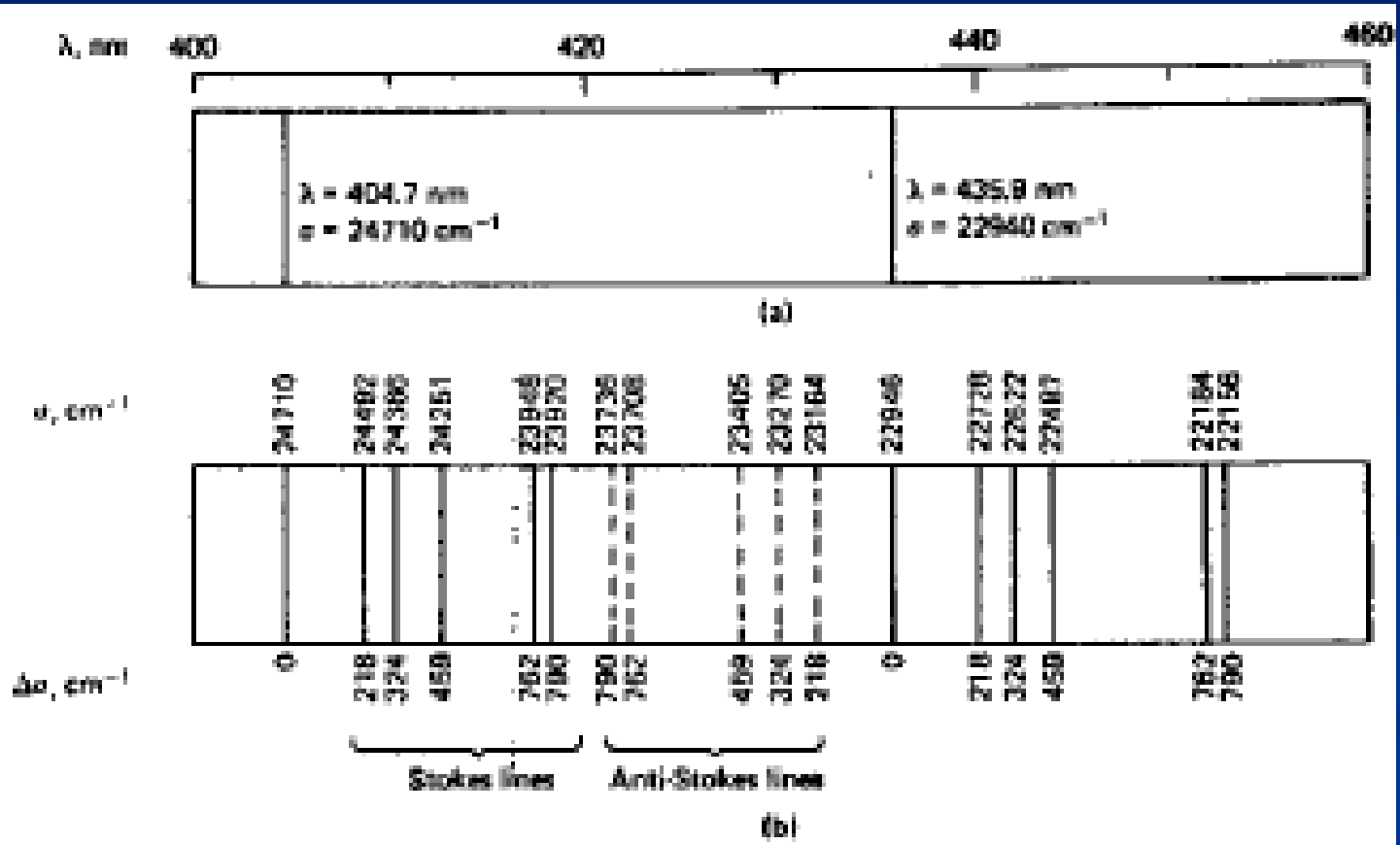

FIGURE 9-1 (a) Intense lines of a mercury arc spectrum and (b) Raman spectrum for CCl_4.

Skoog, West

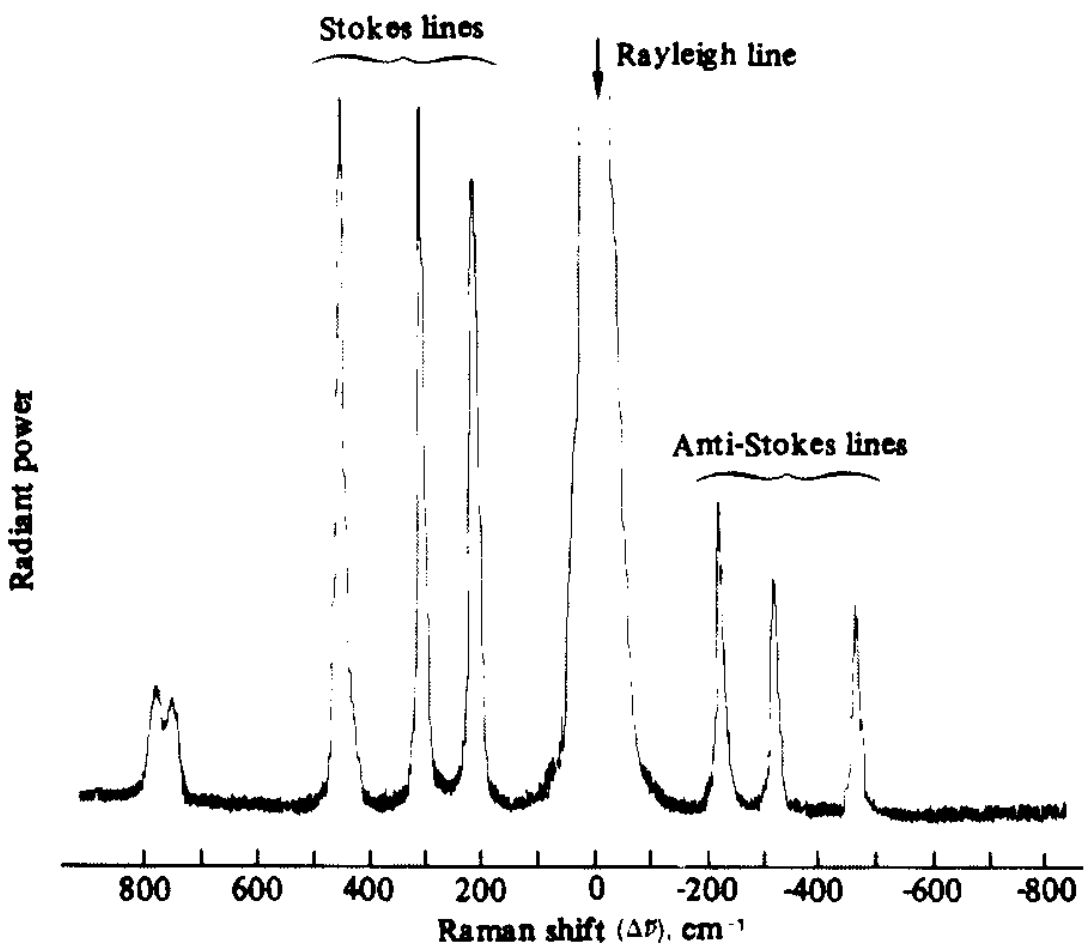

FIGURE 16-6 Raman spectrum of pure carbon tetrachloride. This spectrum was obtained with an He-Ne laser and 3 μL of sample. The Raman shift ($\Delta\bar{\nu}$) is the difference in wavenumbers between the Rayleigh line and the Raman line. [Redrawn with permission from B. J. Bulkin, *J. Chem. Educ.*, *46*, A781 (1969).]

Please note that

For a given molecule the energy shifts observed in a Raman experiment should be identical to the energies of its infrared absorption bands, provided that the vibrational modes involved are active toward both infrared absorption and Raman scattering.

Skoog , West

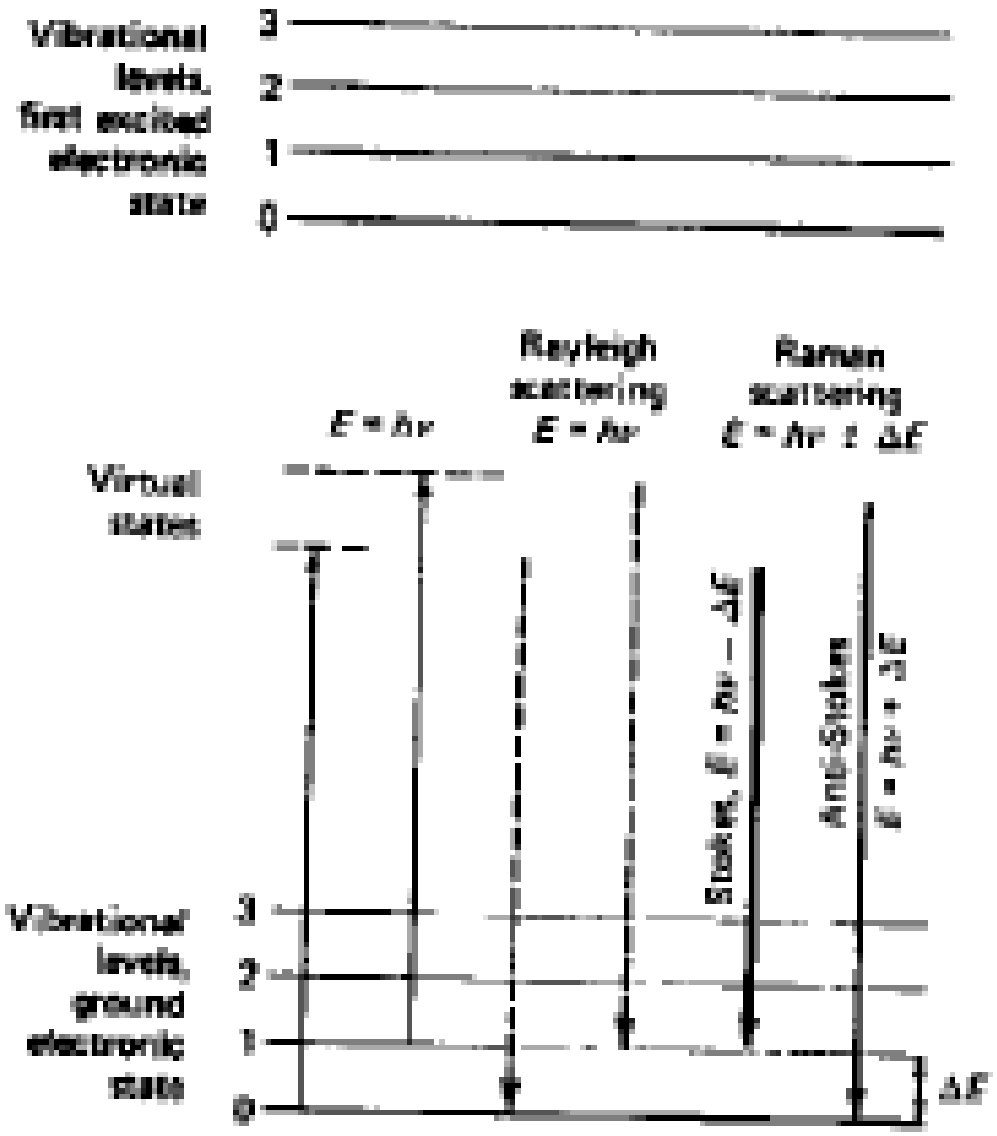

FIGURE 9-2 Origin of Raman spectra.

Skoog, West

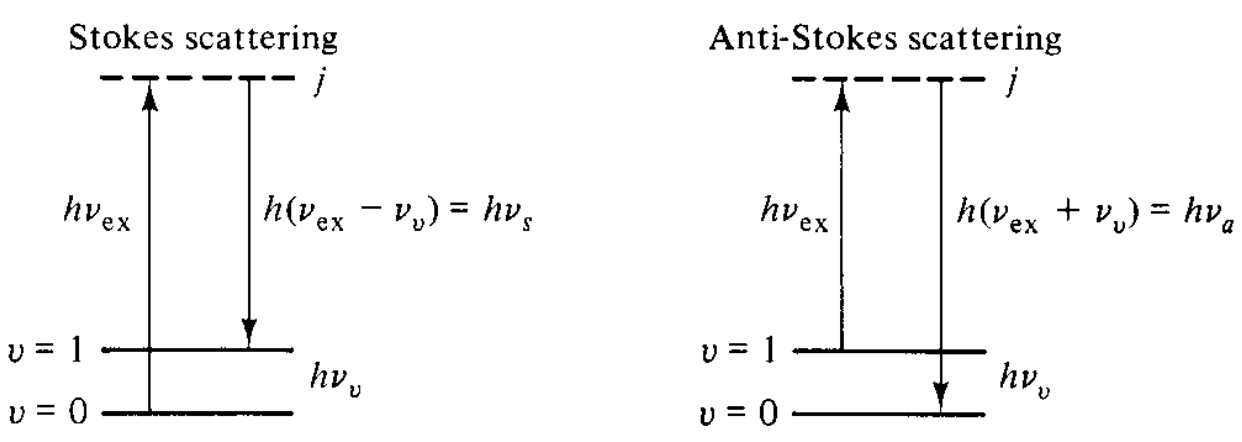
Stokes scattering
j
$h\nu_{ex}$
$h(\nu_{ex} - \nu_v) = h\nu_s$
v = 1
v = 0
$h\nu_v$
Anti-Stokes scattering
j
$h\nu_{ex}$
$h(\nu_{ex} + \nu_v) = h\nu_a$
v = 1
v = 0
$h\nu_v$

(a)

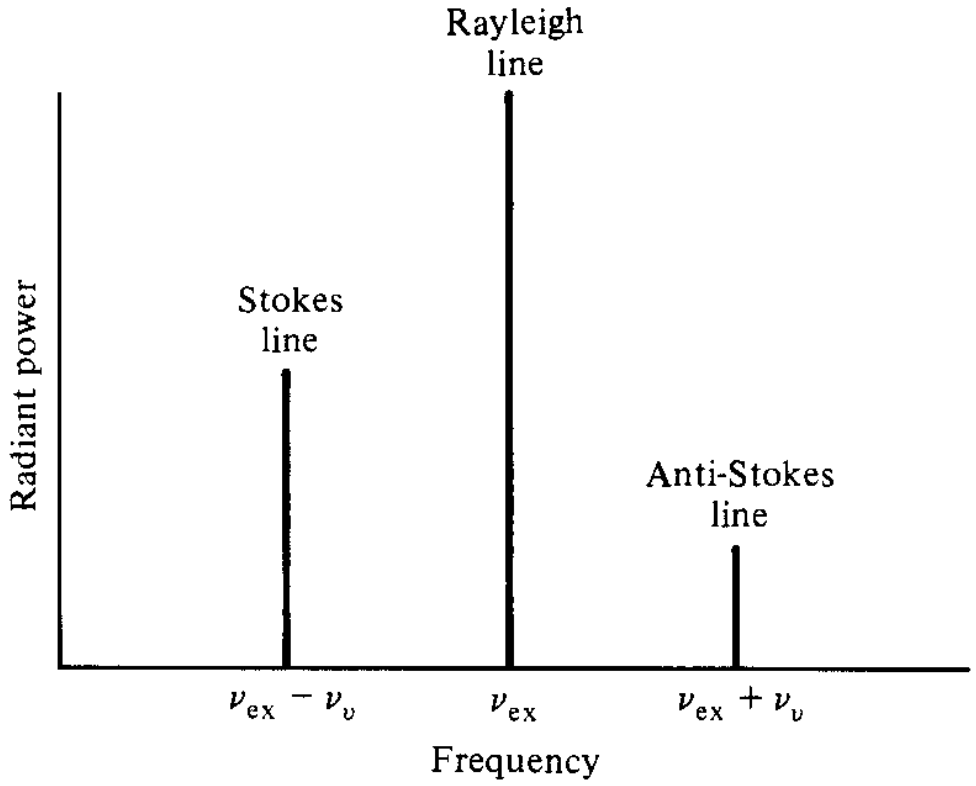
Rayleigh line
Stokes line
Anti-Stokes line
Radiant power
$\nu_{ex} - \nu_v$
ν_{ex}
$\nu_{ex} + \nu_v$
Frequency

(b)

FIGURE 16-5 Energy-level diagram illustrating Raman scattering (a) and resulting Raman spectrum (b). In (a), molecules in the ground vibrational state ($v = 0$) can absorb a photon of energy $h\nu_{ex}$ and reemit a photon of energy $h(\nu_{ex} - \nu_v)$. Molecules in a vibrationally excited state can scatter inelastically and return to the ground state, producing a Raman effect with energy $h(\nu_{ex} + \nu_v)$. The lower-frequency transition is called Stokes scattering, while the higher-frequency transition is called anti-Stokes scattering. We will often label the Stokes frequency ν_s and the anti-Stokes frequency ν_a. If the system is in thermal equilibrium, the equilibrium populations of the ground and excited states follow a Boltzmann distribution. Because the ground-state population is greater than that of the excited state, the Stokes lines are more intense than the anti-Stokes lines (b).

Theory

$$\mathbf{E} = \mathbf{E}_m \cos(2\pi\nu_{ex}t) \qquad (16\text{-}2)$$

Induced dipole moment:

$$\mu_{in} = \alpha\mathbf{E} = \alpha\mathbf{E}_m \cos(2\pi\nu_{ex}t) \qquad (16\text{-}3)$$

where μ_{in} has the units of C m, and α is the polarizability of the sample molecules in J^{-1} C^2 m^2. To obtain the polarizability α' in cubic meters, α must be divided by $4\pi\varepsilon_0$ (i.e., $\alpha = 4\pi\varepsilon_0\alpha'$).

The Raman effect results from the interaction of the polarizability with the normal modes of vibration of the molecules. The polarizability varies with internuclear separation around its equilibrium value α_0 according to

$$\alpha = \alpha_0 + (r - r_e)\left(\frac{\partial\alpha}{\partial r}\right)_e + \cdots \qquad (16\text{-}4)$$

Theory , continued

equilibrium position. The change in internuclear distance varies with the frequency of the vibration ν_v according to

$$r - r_e = r_m \cos(2\pi\nu_v t) \qquad (16\text{-}5)$$

$$\alpha = \alpha_0 + \left(\frac{\partial\alpha}{\partial r}\right)_e r_m \cos(2\pi\nu_v t) \qquad (16\text{-}6)$$

$$\mu_{in} = \alpha_0 \mathbf{E}_m \cos(2\pi\nu_{ex} t) + \frac{\mathbf{E}_m}{2} r_m \left(\frac{\partial\alpha}{\partial r}\right)_e \cos 2\pi(\nu_{ex} + \nu_v)t$$

$$+ \frac{\mathbf{E}_m}{2} r_m \left(\frac{\partial\alpha}{\partial r}\right)_e \cos 2\pi(\nu_{ex} - \nu_v)t \qquad (16\text{-}8)$$

Requirements for Raman Scattering.

$$R = \int \psi_i^* \left[\alpha_0 + (r - r_e) \left(\frac{\partial \alpha}{\partial r} \right)_e \right] \psi_j \, d\tau \qquad (16\text{-}9)$$

$$R = \int \psi_i^* \left[(r - r_e) \left(\frac{\partial \alpha}{\partial r} \right)_e \right] \psi_j \, d\tau \qquad (16\text{-}10)$$

From equation 16-10 it is clear that there must be a *change in polarizability* during the vibration in order for Raman scattering to occur. The selection rules further predict that Raman lines, corresponding to fundamental modes, occur with $\Delta v = \pm 1$. Just as in IR spectroscopy, overtone transitions, which are much weaker, appear at $\Delta v = \pm 2$.

Raman Spectroscopy: Classical Treatment

- Number of peaks related to degrees of freedom

  DoF = 3N - 6 (bent) or 3N - 5 (linear) for N atoms

- Energy related to harmonic oscillator

$$\sigma \text{ or } \Delta\sigma = \frac{c}{2\pi}\sqrt{\frac{k(m_1+m_2)}{m_1 m_2}}$$

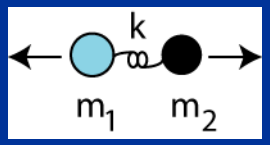

- Selection rules related to symmetry

  Rule of thumb: symmetric=Raman active, asymmetric=IR active

CO_2	H_2O
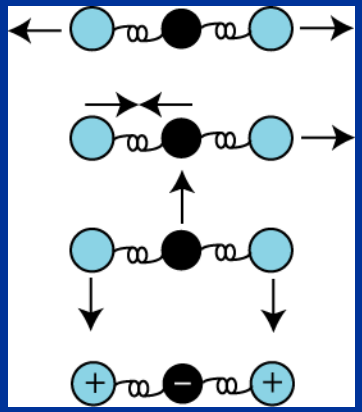	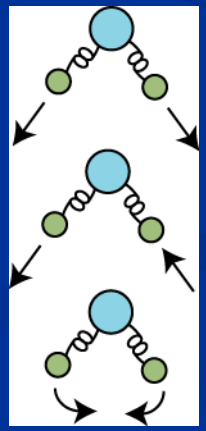
Raman: 1335 cm^{-1}	Raman + IR: 3657 cm^{-1}
IR: 2349 cm^{-1}	Raman + IR: 3756 cm^{-1}
IR: 667 cm^{-1}	Raman + IR: 1594 cm^{-1}

dts@u.washington.edu

Examples of Raman active and inactive vibrations in CO2

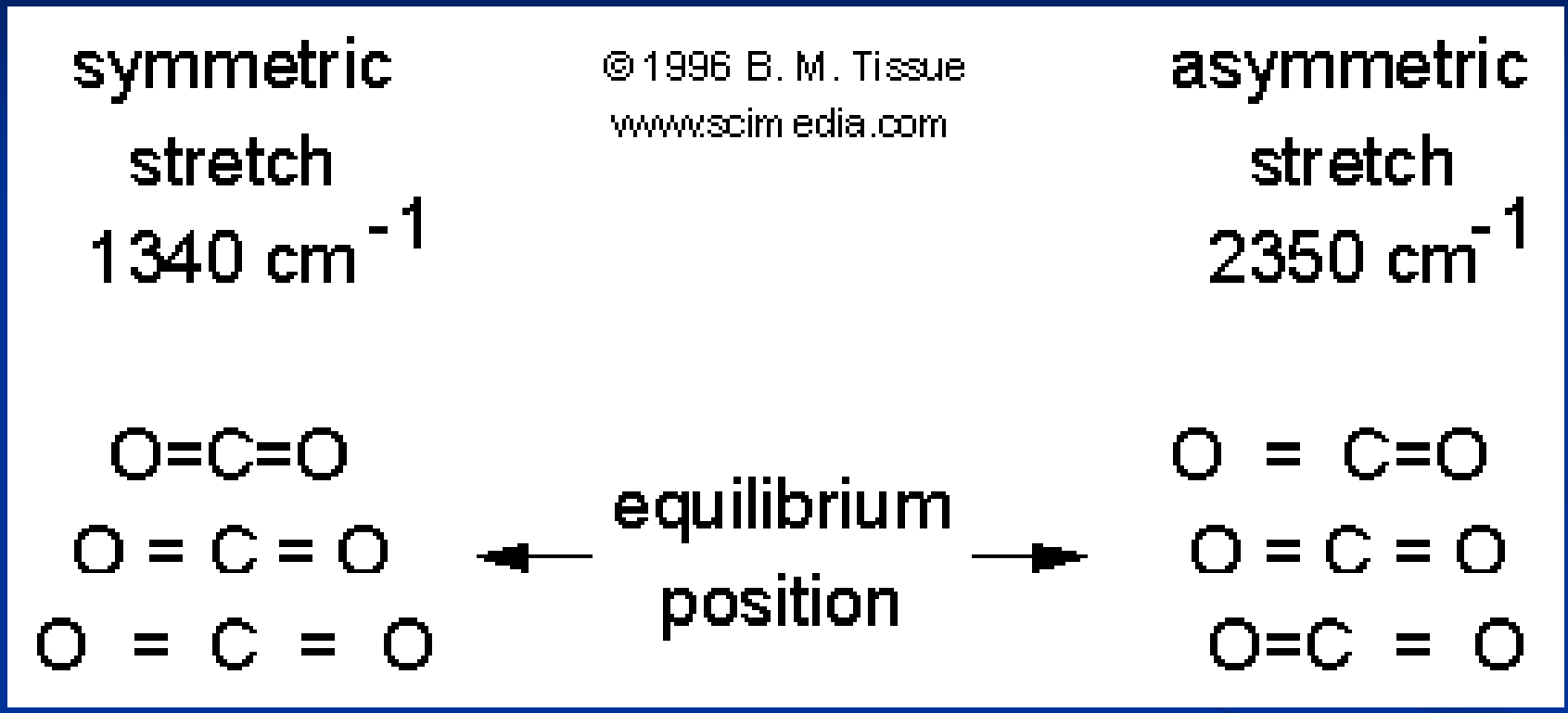

The result is that there must be a change in polarizability during the vibration for that vibration to inelastically scatter radiation

dts@u.washington.edu

Using the group theory

An easy way to determine whether a transition is allowed or not in IR and Raman spectroscopy is to use group theory and the symmetry properties of the states and the operator (dipole moment or polarizability) involved. For integrals

Molecules with center of symetry

For molecules with a center of symmetry, these differences lead to the conclusion that there are no IR active transitions in common with Raman active transitions, the **mutual exclusion principle**. For example, the symmetric stretching mode of CO_2 is IR inactive because there is no dipole moment change during the vibration (recall Figure 14-1). On the other hand, the polarizability varies during the vibration, which leads to Raman activity. For the asymmetric stretch of CO_2, the dipole moment changes during the vibration. However, as the polarizability of one of the C—O bonds increases as it lengthens, that of the other decreases, and overall, there is no change. Thus the asymmetric stretching vibration of CO_2 is Raman inactive.

Noncentrosymetric Molecules

For noncentrosymmetric molecules, there are many cases in which the mutual exclusion principle still holds. However, many other vibrational modes may be both Raman and IR active. One interesting case is that of C_1 symmetry, in which there is no symmetry. Here all vibrations are both Raman and IR active. In cases where vibrations are Raman and IR active, the intensities observed for the same vibration may be quite different.

Raman Spectroscopy: General

- IR and Raman are both useful for Fingerprinting

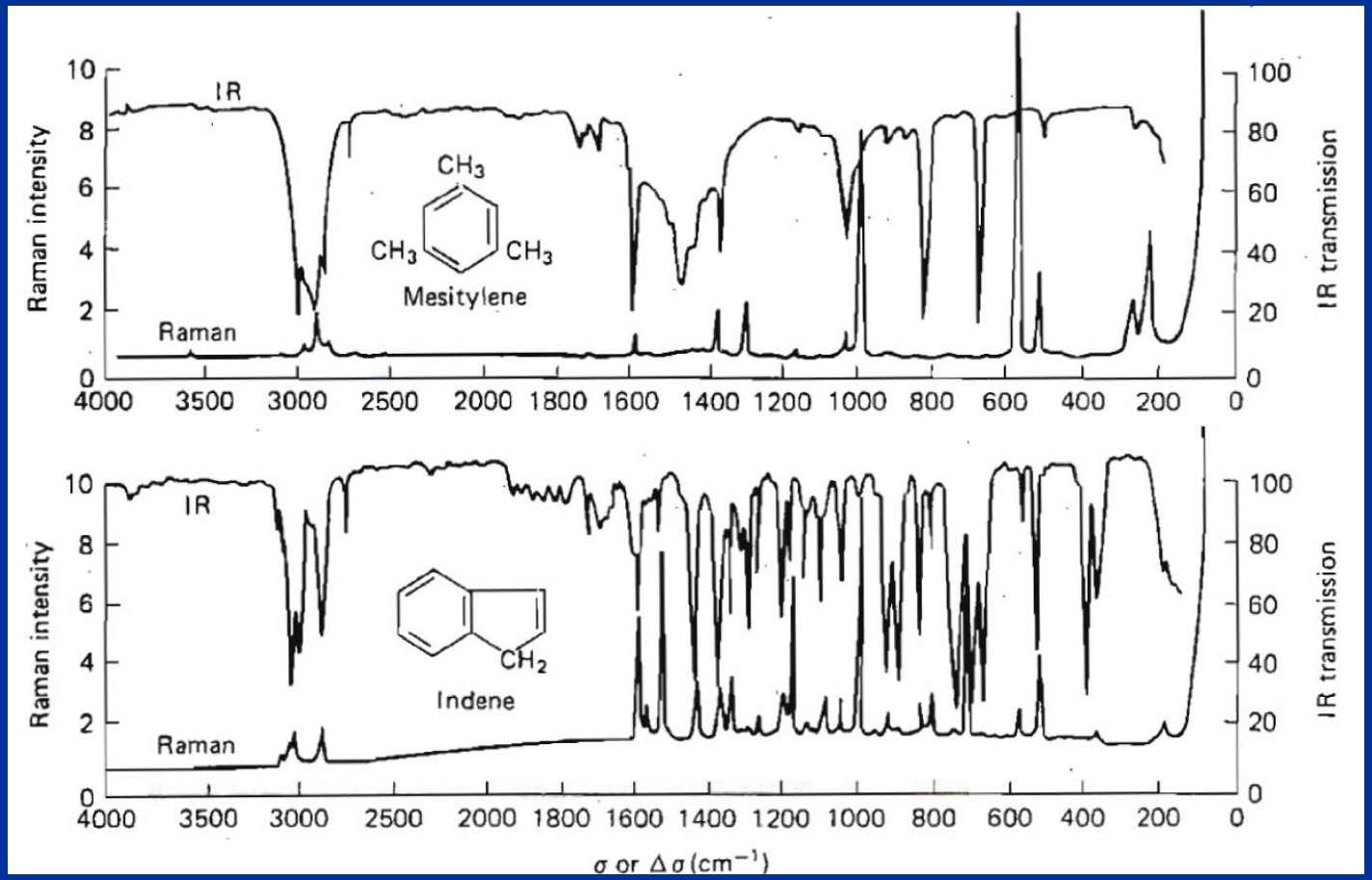

- Symmetry dictates which are active in Raman and IR

dts@u.washington.edu

Raman Intensities.

$$\Phi_R \propto \sigma(\nu_{ex})\nu_{ex}^4 E_0 n_i e^{-E_i/kT} \qquad (16\text{-}11)$$

where $\sigma(\nu_{ex})$ is the Raman cross section in cm^2, n_i is the number density in state i, and the exponential term is the Boltzmann factor for state i. Typically, $\sigma(\nu_{ex})$ is on the order of 10^{-29} cm^2 for a good Raman scatterer.

Depolarization ratio

an additional factor, called the **depolarization ratio**, that is useful in structure elucidation. If the incident beam is polarized, as it is with a CW laser source, the Raman-scattered radiation can be polarized to various degrees that depend on the nature of the active vibration.

where $(\Phi_R)_\perp$ is the Raman radiant power polarized perpendicular to the polarization of the original beam and $(\Phi_R)_\parallel$ is that polarized parallel to the original beam.

The depolarization ratio can give information about the symmetry of the vibration involved. For example, if the molecule is approximately spherical and the vibration is totally symmetric, the incident beam polarization is maintained; the depolarization ratio would be very small in this case. On the other hand, if the vibration distorts the symmetry, or if the molecule is not symmetric to begin with, a significant depolarization can occur. From scattering theory, it is predicted that for nonsymmetric vibrations $\rho = 0.75$, while for symmetric vibrations $\rho < 0.75$. With CCl_4, for example, the 459-cm^{-1} Raman line has a value of $\rho = 0.005$. This line arises from the totally symmetric breathing vibration; the four chlorine atoms move simultaneously away and toward the central carbon atom. The lines at 218 and 314 cm^{-1}, however, arise from nonsymmetric vibrations; for these, $\rho \approx 0.75$.

$$\rho = \frac{(\Phi_R)_\perp}{(\Phi_R)_\parallel}$$

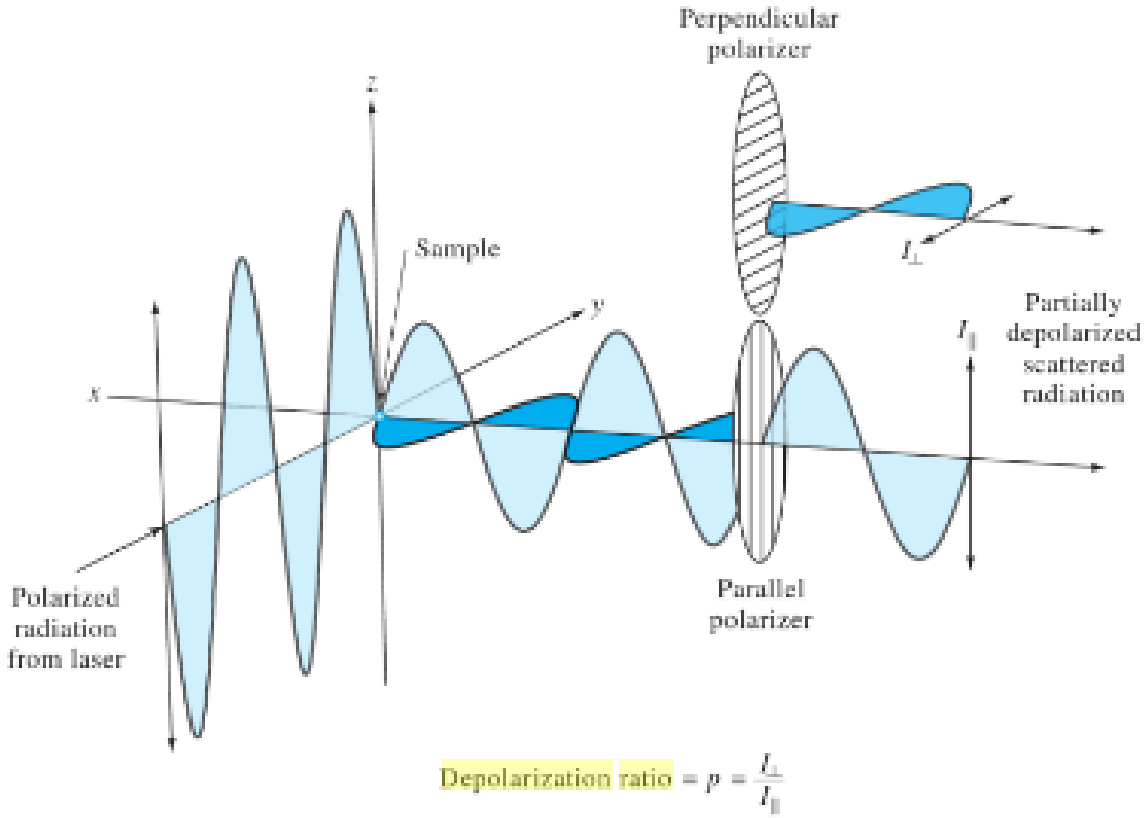

$$\text{Depolarization ratio} = p = \frac{I_\perp}{I_\parallel}$$

FIGURE 18-5 Depolarization resulting from Raman scattering.

Instrumentation

A Raman system typically consists of four major components:

1. Excitation source (Laser).
2. Sample illumination system and light collection optics.
3. Wavelength selector (Filter or Spectrophotometer).
4. Detector (Photodiode array, CCD or PMT).

A sample is normally illuminated with a laser beam in the ultraviolet (UV), visible (Vis) or near infrared (NIR) range. Scattered light is collected with a lens and is sent through interference filter or spectrophotometer to obtain Raman spectrum of a sample.

Instrumentation

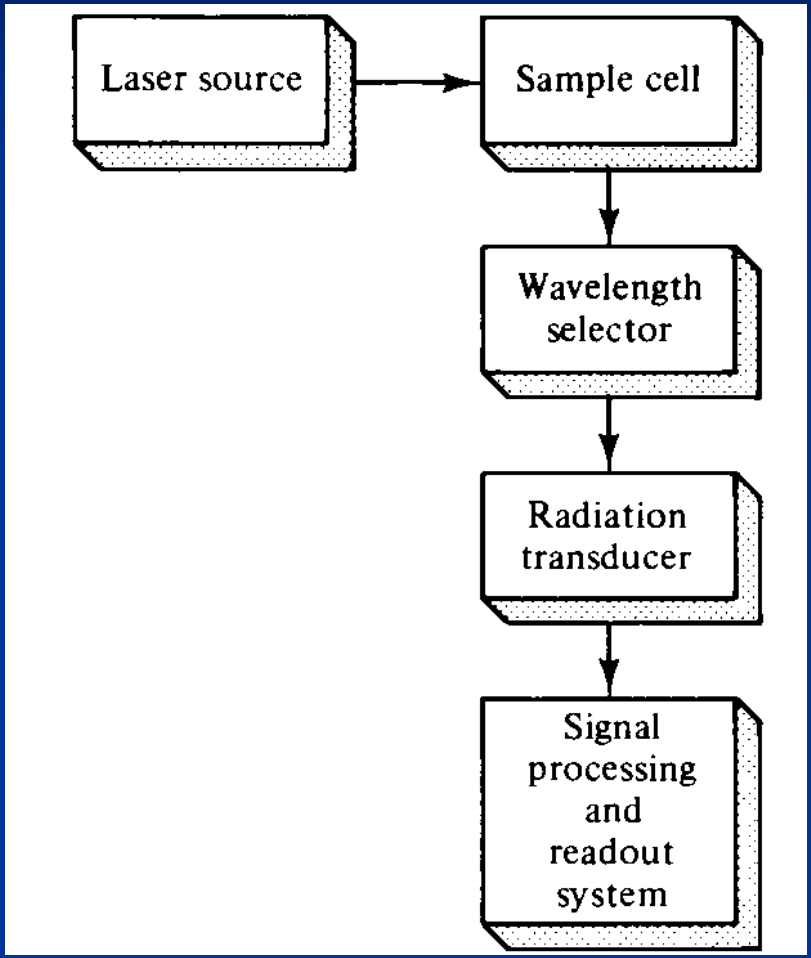

FIGURE 16-7 Block diagram of a Raman spectrometer. The laser source radiation is directed into a sample cell. The Raman scattering is normally observed at right angles to avoid directly viewing the source radiation. A wavelength selector isolates the spectral region of interest. The radiation transducer converts the radiant power or photon flux into a dc electrical signal or a count rate.

Sources

TABLE 16-2

Laser excitation wavelengths

Laser type	Wavelengths (nm)
He-Ne	632.8
Ar^+	488.0, 514.5
Kr^+	530.9, 647.1

Sample Cells and Cell Configurations.

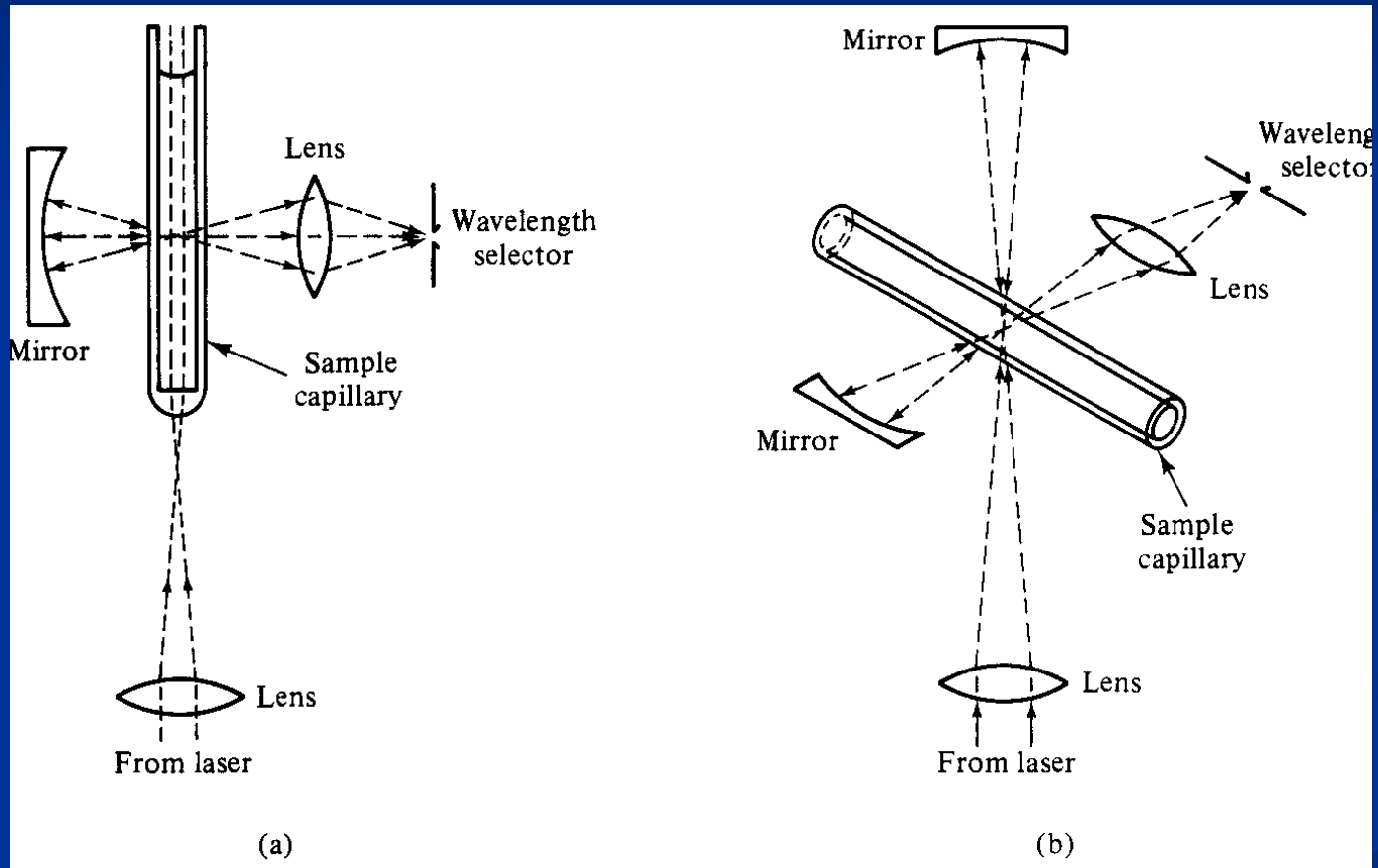

FIGURE 16-8 Cell configurations for Raman spectra of micro samples.

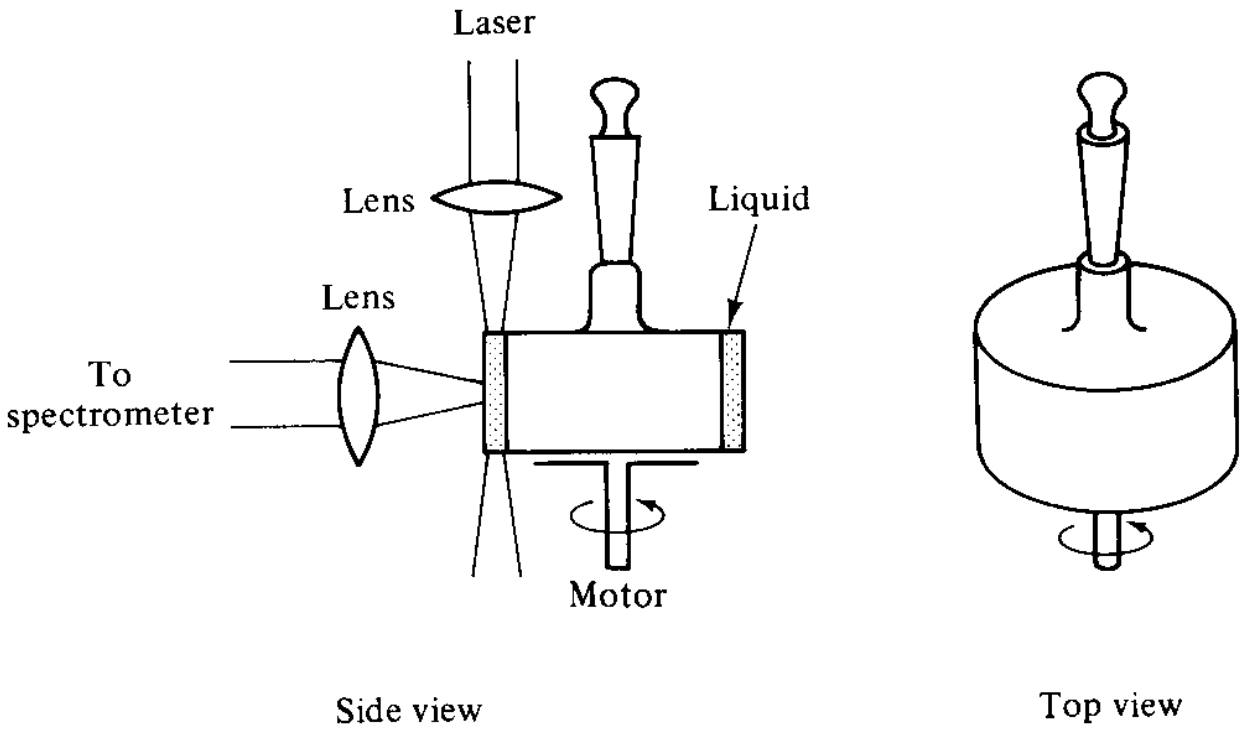

FIGURE 16-9 Rotating cell for Raman spectroscopy of highly colored solutions. By spinning the sample in the laser beam, intense, localized overheating of the sample is avoided. Thus spectra can be obtained on highly absorbing solutions.

Samples: Gas, liquid, solid

The Raman Microprobe.

The Raman Microprobe. The Raman microprobe is a instrument that couples a Raman spectrometer with an optical microscope. This allows the ex-

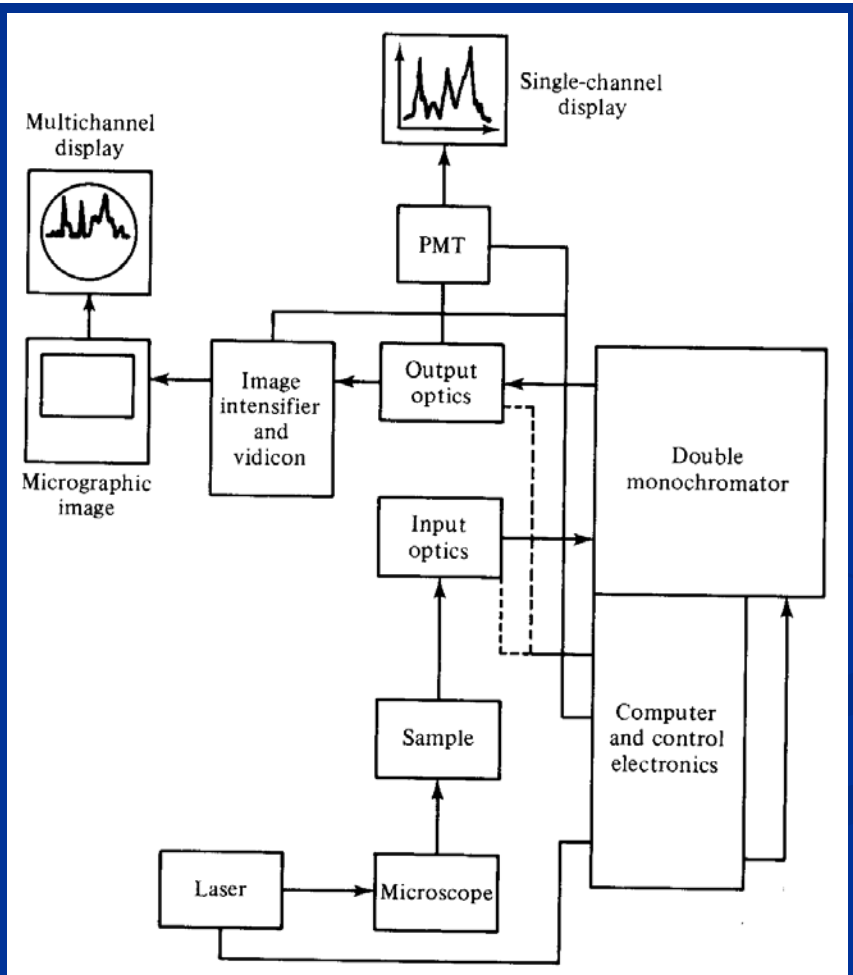

FIGURE 16-11 Example of an application of the Raman microprobe. In (a) a sample is placed on the microscope slide and photographed (left). On the right is the total Raman spectrum taken from the entire field of view. This spectrum shows that the particles are TiO_2 and $SrSO_4$. In (b)

Part of figure 16-11

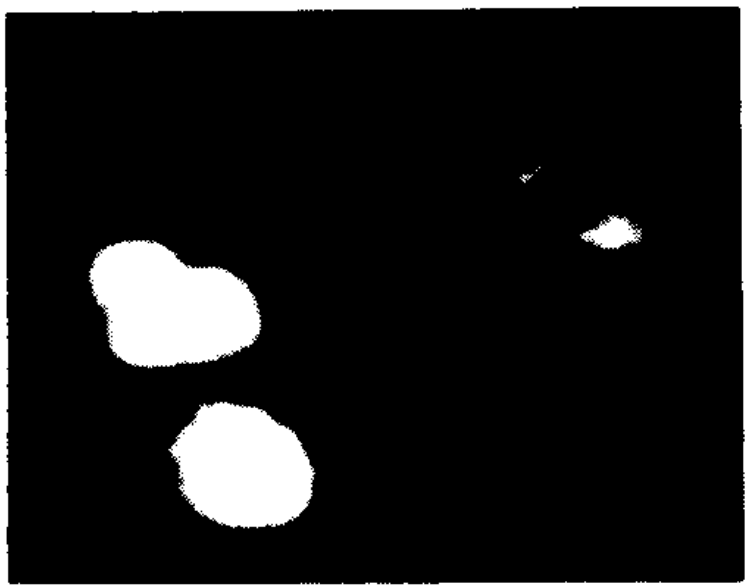

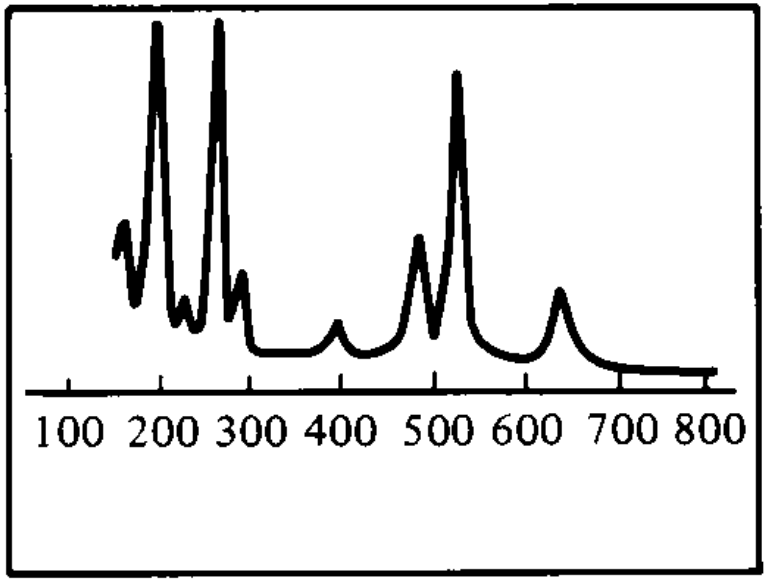

(a)

Raman mapping

Applications, examples

Characterization of Carbon Nanotubes by Raman spectroscopy

S. Costa[1], E. Borowiak-Palen[*1], M. Kruszyñska[1], A. Bachmatiuk[1], R J. Kaleńczuk[1]

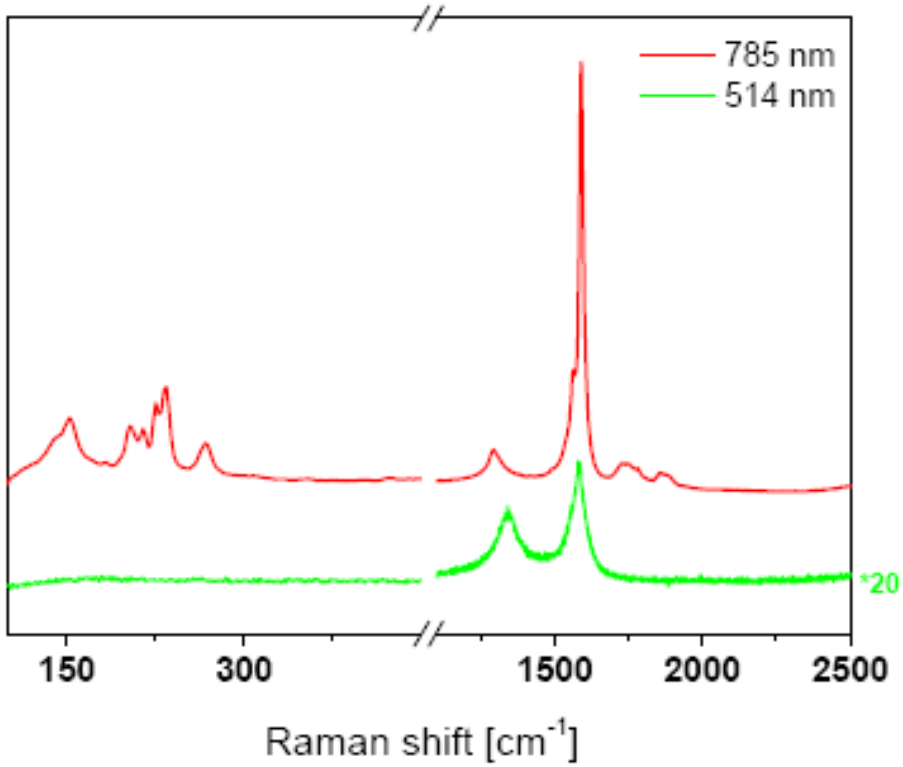

Fig. 1- (a) Different Raman spectra of SWCNT obtained from red laser (785 nm) and green laser (514

Raman Spectroscopy: Dan's trip to NTUF

Flow Field Plate - Graphite

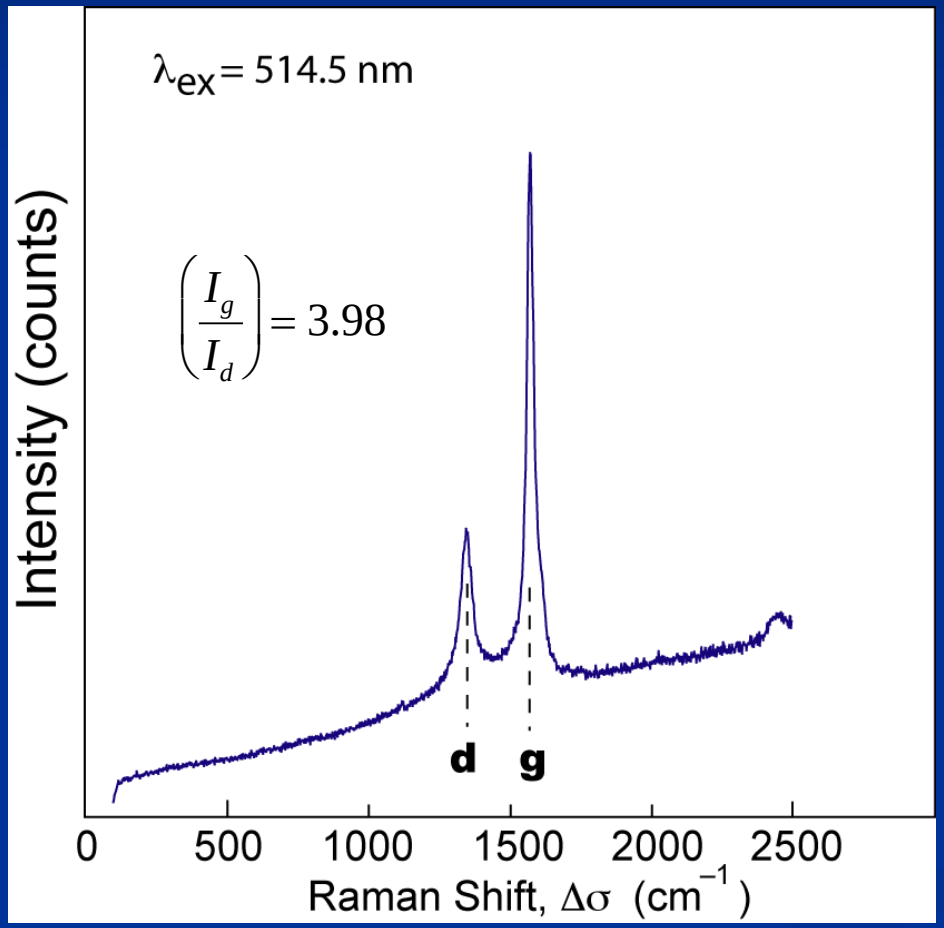

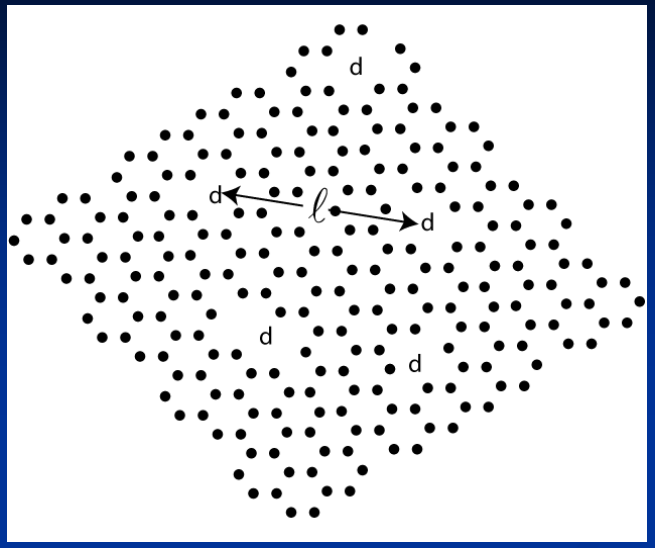

Nanocrystalline graphite has graphitic (**g**) and disorder (**d**) peaks. The characteristic dimension of graphitic domains is given by:

$$L_a(\text{Å}) = 44\left(\frac{I_g}{I_d}\right)$$

$$L_a = 175\text{Å}$$

From early literature on graphitic materials
Tuinstra and Koenig, J. Chem Phys. 53, 1126 (1970).

Raman Spectroscopy: Dan's trip to NTUF

Gas Diffusion Layers (graphite paper)

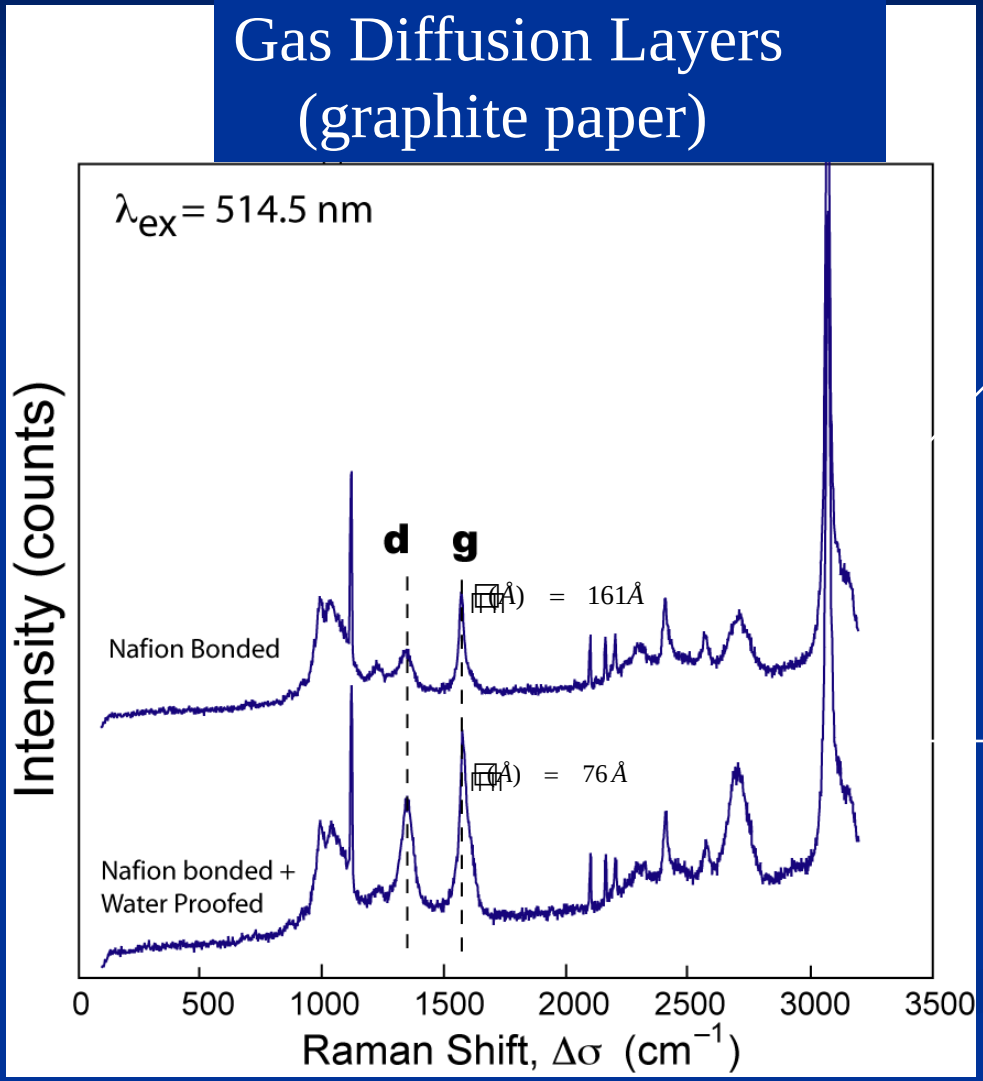

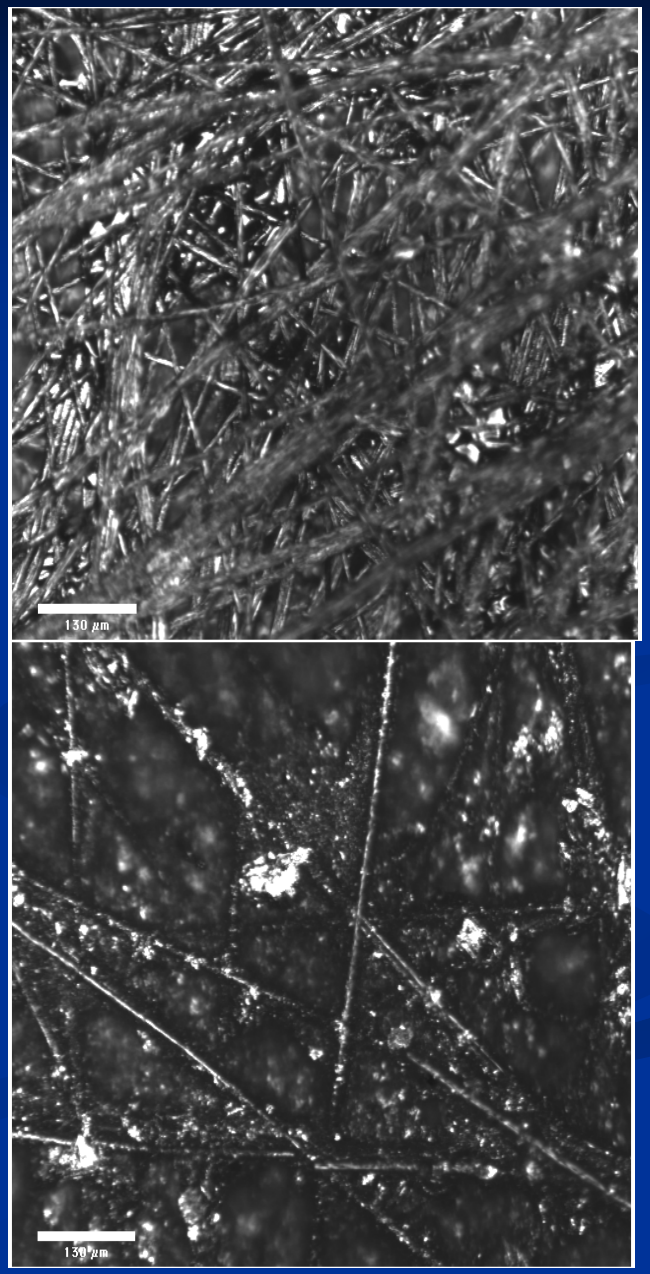

Comparison of Raman and IR Spectrometry

Comparison

Advantages

(Home work)

Raman and IR spectrometry should be viewed as complementary techniques particularly for structural studies.

Resonance Raman Spectroscopy

In resonance Raman spectroscopy, the energy of the incoming laser is adjusted such that it or the scattered light coincide with an electronic transition of the molecule or crystal. When the frequency of the laser beam is tuned to be near an electronic transition (resonance), the vibrational modes associated with that particular transition exhibit a greatly increased Raman scattering intensity. This usually overwhelms Raman signals from all of the other transitions. For instance, resonance with a π-π* transition enhances stretching modes of the π-bonds involved with the transition, while the other modes remain unaffected.

Raman and Flourescence

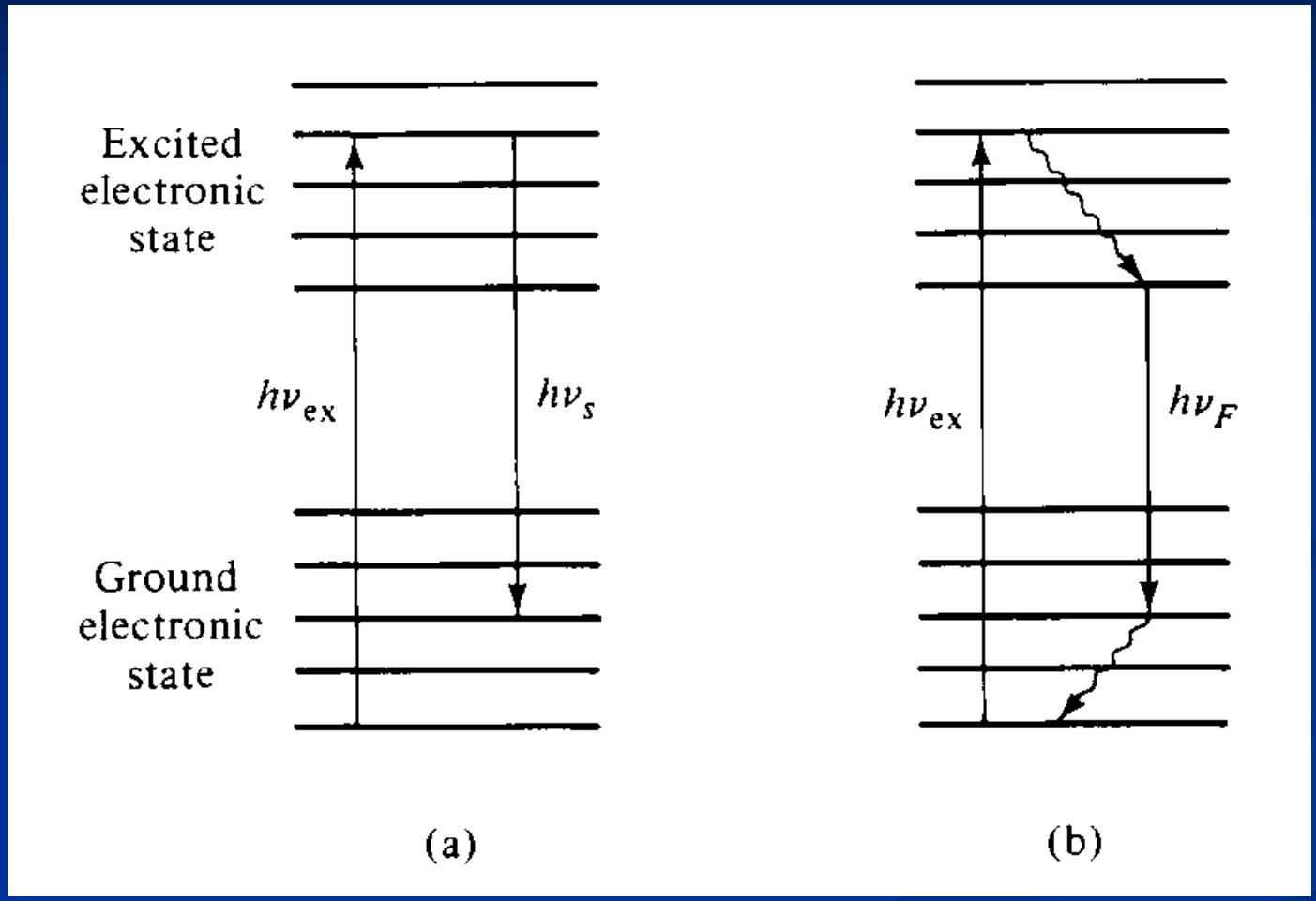

FIGURE 16-12 Energy-level diagrams illustrating resonance Raman scattering for an overtone transition (a) and fluorescence emission (b). In

Continued…

Example

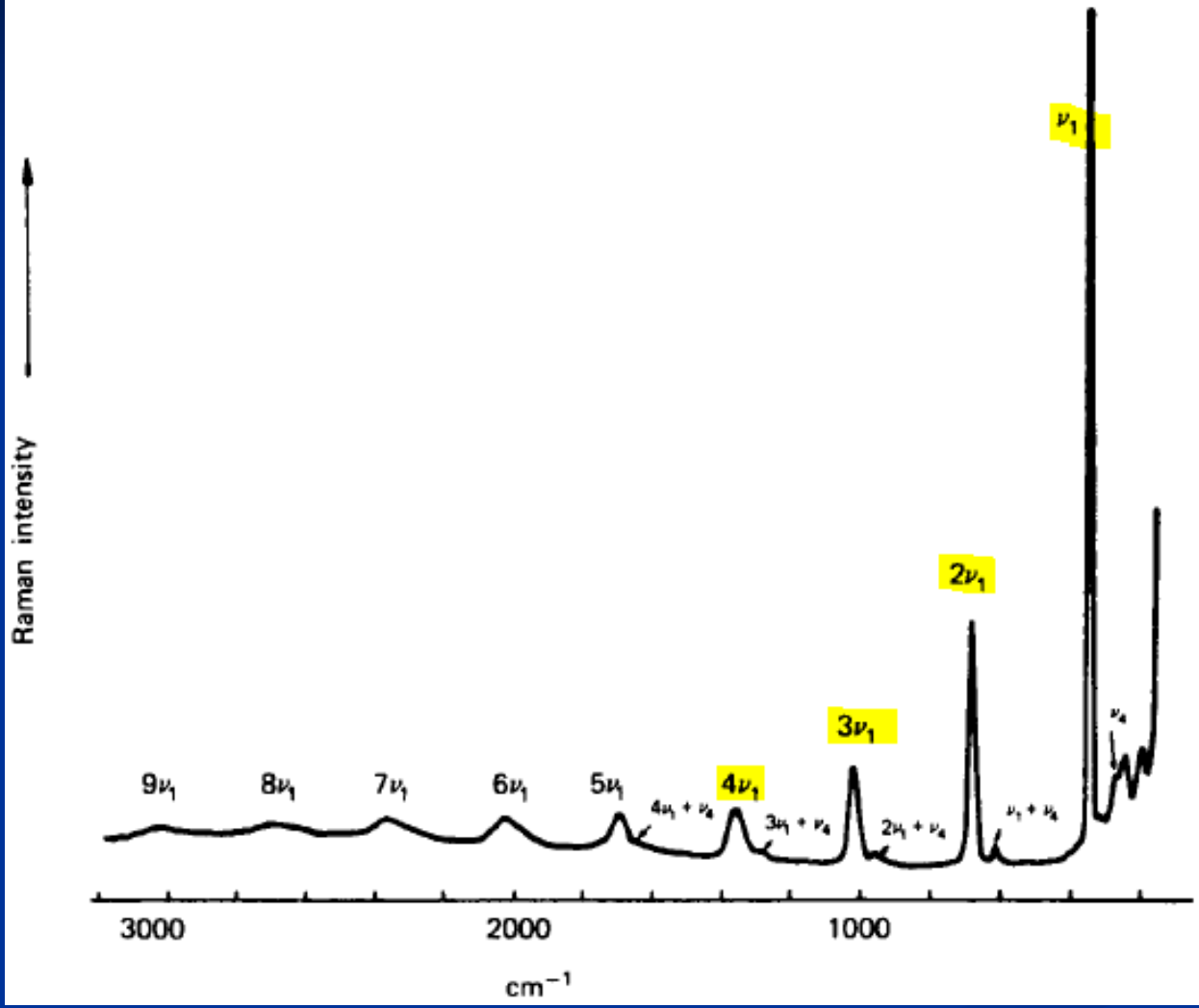

به افزایش شدت اورتونهای ارتعاش اصلی Mo-Mo توجه کنید

FIGURE 16-14 Resonance Raman spectrum of $Cs_4Mo_2Cl_8$. The exciting frequency was brought into coincidence with the electronic transition involving the δ electron of the Mo–Mo bond. This results in resonance enhancement of the totally symmetric Mo–Mo vibration. Note the overtone progression of the Mo–Mo fundamental. [Reprinted with permission from R. J. H. Clark and M. L. Franks, *J. Chem. Soc. Chem. Commun.*, 9, 316 (1974).]

Raman and Flourescence

. The fluorescence appears as a broadband background signal, which can obscure the resonance Raman signals. The resonance Raman signals can be enhanced relative to fluorescence signals by time-resolution techniques. The resonance Raman process is nearly instantaneous compared to the much slower fluorescence emission.

16-4 LASER SCATTERING METHODS

Radiation scattering methods have been widely used for many years in the determination of molecular weights, particles sizes, and particles shapes. Several commercial instruments, called light-scattering photometers, are available for such measurements. Many of these are similar in design to the photometer shown in Figure 16-17.

FIGURE 16-17 Light-scattering photometer. In (a), collimated radia-

Continued...

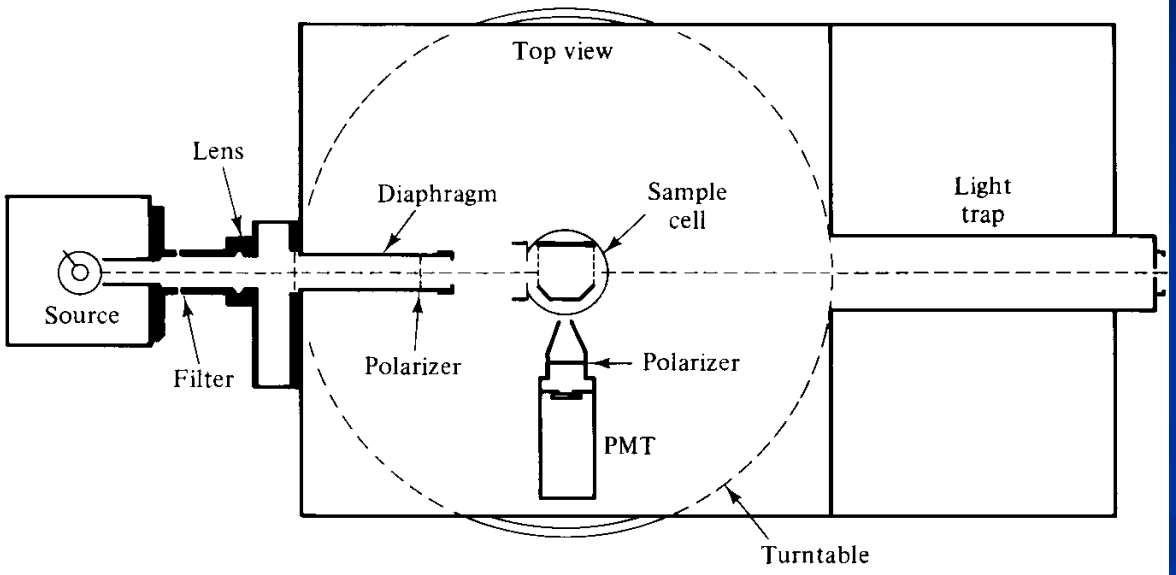

(a)

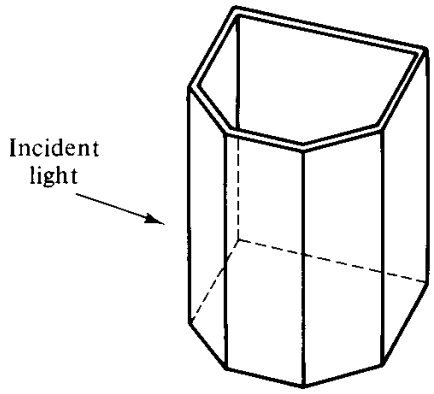

(b)

Molecular Weight Determinations

Consider again equation 16-1

Let us consider the sample to be a collection of isotropic polarizable particles (e.g., molecules). The polarizability α' is directly proportional to molecular weight [$\alpha' \approx M\eta_0(d\eta/dc)/(2\pi N)$], where M is the molecular weight, N is Avogadro's number, η_0 is the refractive index of the pure solvent, and $d\eta/dc$ is the refractive index change of the solution with concentration. Hence the intensity of Rayleigh scattering from a single particle is proportional to the square of the molecular weight.

TURBIDIMETRY AND NEPHELOMETRY

Turbidimetry and **nephelometry** are methods that measure the concentrations of particulate matter in a suspension. Both are based on the elastic scattering of radiation. Turbidimetric methods measure the decrease that occurs in the transmitted radiation as a result of particle scattering, while nephelometric methods measure the radiant power of the scattered radiation itself.

The scattering of radiation by suspended particles is often called the **Tyndall effect**. In the UV and visible regions the scattering particles are usually of colloidal size, from 1 nm to 1 μm in diameter. The scattering can be Rayleigh, Debye, or Mie, depending on the size of the particles.

TURBIDIMETRY AND NEPHELOMETRY

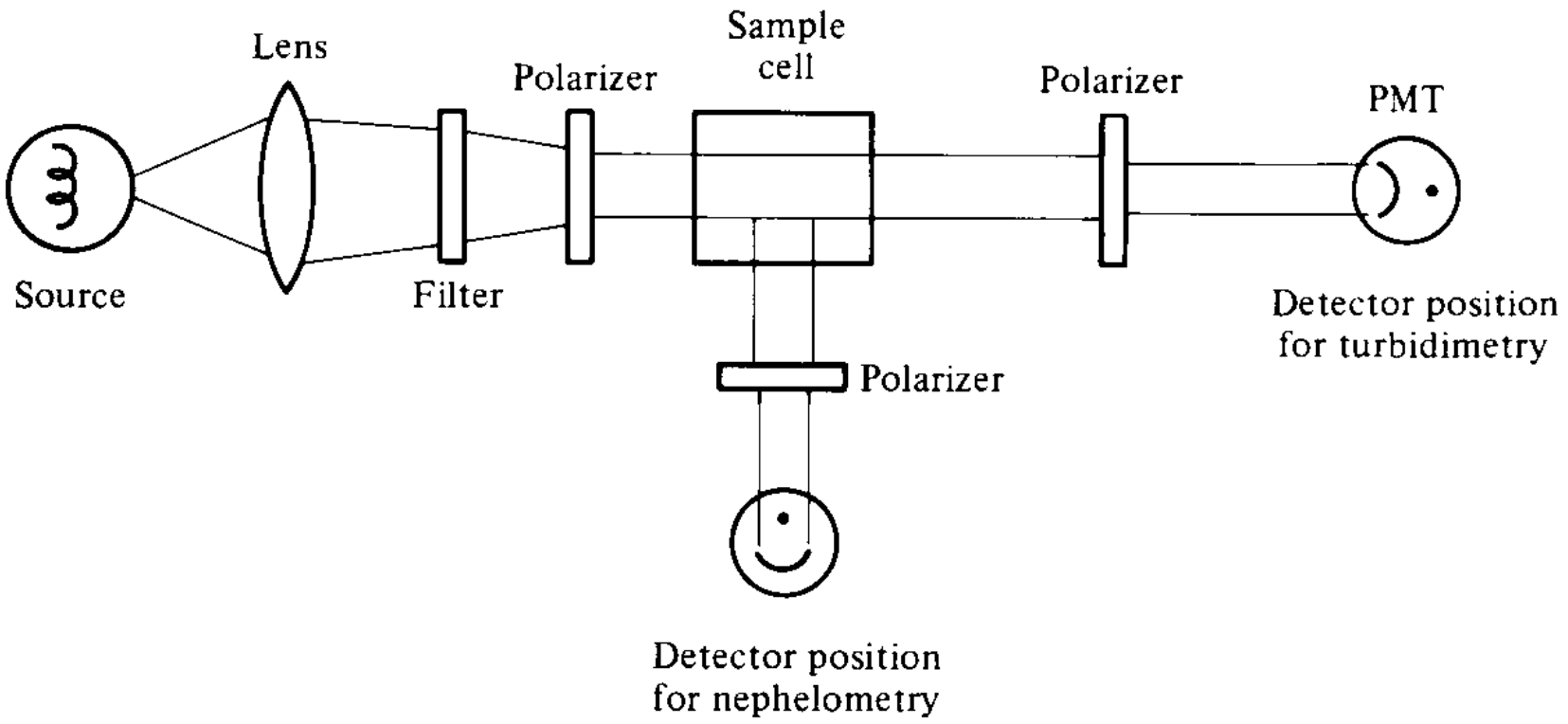

FIGURE 16-16 Instrumentation for turbidimetry and nephelometry. In turbidimetry the detector is placed in line with the source, while in nephelometry a 90° configuration is employed. In some instruments, polar-

TURBIDIMETRY AND NEPHELOMETRY

TABLE 16-3

Turbidimetric and nephelometric methods

Species	Particles formed	Reagent	Method[a]
Ag	AgCl	NaCl	T, N
As	As	KH_2PO_2	T
Au	Au	$SnCl_2$	T
Ca	CaC_2O_4	$H_2C_2O_4$	T
Cl^-	AgCl	$AgNO_3$	T, N
K	$K_2NaCo(NO_2)_6$	$Na_3Co(NO_2)_6$	T
SO_4^{2-}	$BaSO_4$	$BaCl_2$	T, N
Se	Se	$SnCl_2$	T
Te	Te	NaH_2PO_2	T

16-5 REMOTE SENSING WITH LASERS

To determine the optical characteristics of the atmosphere,….

Many of the laser-based methods in such studies are based on radiation scattering.

Many of theses are called **laser radar** or **lidar** methods.

Following the introduction of lasers in the 1960s, it was soon realized that these sources allow optical measurements to be made at sites remote from the probed area.

For example, it is now common to obtain information on the particulate and aerosol content of the atmosphere using lidar. Particle sizes can readily be determined from Mie scattering. Multiwavelength lidar has been employed to obtain aerosol size distributions.